Glycobiology, 2023, **33**, 4, 301–310
https://doi.org/10.1093/glycob/cwad006
Advance access publication date 31 January 2023
Original Article

O-fucosylation of thrombospondin type I repeats is dispensable for trafficking thrombospondin 1 to platelet secretory granules

Steven J. Berardinelli[1], Andrew R. Sillato[2], Richard C. Grady[2], Sanjiv Neupane[2], Atsuko Ito[1], Robert S. Haltiwanger[1,*], Bernadette C. Holdener[2,*]

[1]Complex Carbohydrate Research Center, Department of Biochemistry and Molecular Biology, University of Georgia, Athens, GA 30602, USA, [2]Department of Biochemistry and Cell Biology, Stony Brook University, Stony Brook, NY 11794, USA

*Corresponding authors: E-mail: rhalti@uga.edu; bernadette.holdener@stonybrook.edu

Thrombospondin 1 (THBS1) is a secreted extracellular matrix glycoprotein that regulates a variety of cellular and physiological processes. THBS1's diverse functions are attributed to interactions between the modular domains of THBS1 with an array of proteins found in the extracellular matrix. THBS1's three Thrombospondin type 1 repeats (TSRs) are modified with *O*-linked glucose-fucose disaccharide and *C*-mannose. It is unknown whether these modifications impact trafficking and/or function of THBS1 in vivo. The *O*-fucose is added by Protein *O*-fucosyltransferase 2 (POFUT2) and is sequentially extended to the disaccharide by β3glucosyltransferase (B3GLCT). The *C*-mannose is added by one or more of four *C*-mannosyltransferases. *O*-fucosylation by POFUT2/B3GLCT in the endoplasmic reticulum has been proposed to play a role in quality control by locking TSR domains into their three-dimensional fold, allowing for proper secretion of many *O*-fucosylated substrates. Prior studies showed the siRNA knockdown of *POFUT2* in HEK293T cells blocked secretion of TSRs 1–3 from THBS1. Here we demonstrated that secretion of THBS1 TSRs 1–3 was not reduced by CRISPR-Cas9-mediated knockout of *POFUT2* in HEK293T cells and demonstrated that knockout of *Pofut2* or *B3glct* in mice did not reduce the trafficking of endogenous THBS1 to secretory granules of platelets, a major source of THBS1. Additionally, we demonstrated that all three TSRs from platelet THBS1 were highly *C*-mannosylated, which has been shown to stabilize TSRs in vitro. Combined, these results suggested that POFUT2 substrates with TSRs that are also modified by *C*-mannose may be less susceptible to trafficking defects resulting from the loss of the glucose-fucose disaccharide.

Key words: POFUT2; *O*-fucosylation; *C*-mannosylation; thrombospondin 1; protein trafficking.

Introduction

The secreted, non-structural extracellular matrix glycoprotein thrombospondin 1 (THBS1), also known as the thrombin sensitive protein (TSP1; Baenziger et al. 1971), mediates extracellular matrix organization, bioavailability of growth factors and cytokines, as well as cell–matrix interactions (reviewed in Resovi et al. 2014, Kale et al. 2021). Consistent with the wide range of cellular functions, THBS1 regulates diverse physiological processes including, but not limited to, vascular responsiveness, angiogenesis, platelet activation, inflammation, and cell death, impacting wound healing and tumorigenesis (reviewed in Kale et al. 2021; Resovi 2014). THBS1's diverse functions are attributed to the modular nature of the protein (Lawler 1986). The three thrombospondin type 1 domain repeats (TSRs) mediate interactions with a diversity of proteins including but not limited to the cell surface proteins CD36 and Jagged1, growth factors including TGFβ and VEGFA, structural ECM proteins collagen V and VII, and Fibrinogen/fibrin (Resovi et al. 2014; Kale et al. 2021).

Each of THBS1's TSRs have a consensus site ($C^1XX(S/T)C^2$) for *O*-linked fucosylation by Protein *O*-fucosyltransferase 2 (POFUT2) with subsequent extension to the glucoseβ1–3fucose (glucose-fucose) disaccharide by β3glucosyltransferase (B3GLCT) (Fig. 1A) (Hofsteenge et al. 2001). In contrast to many other glycan modifications that occur in the endoplasmic reticulum (ER), POFUT2 and B3GLCT only recognize and modify properly folded TSRs (Holdener and Haltiwanger 2019). POFUT2 has been proposed to be a folding sensor for TSRs. Results from HPLC based in vitro unfolding and refolding assays demonstrate that the addition of *O*-linked fucose stabilizes the THBS1-TSR3 native fold, with increased stability observed when extended to the glucose-fucose disaccharide (Vasudevan et al. 2015). Recent structural studies reveal that the disaccharide interacts with underlying amino acid side chains, protecting the Cys2-Cys6 disulfide bond in THBS1-TSR3 and preventing reduction (Berardinelli et al. 2022). In HEK293T cell-based secretion assays, knockdown of *POFUT2* or *B3GLCT* using siRNA reduced the secretion of THBS1 TSRs 1–3 (Vasudevan et al. 2015). More recent studies using knockout of *POFUT2* or *B3GLCT* in HEK293T cells using CRISPR-Cas9 showed a reduced secretion of many related proteins containing TSRs (Dubail et al. 2016; Hubmacher et al. 2017; Zhang et al. 2020; Neupane et al. 2021, 2022). These results led to the hypothesis that efficient folding of proteins containing TSRs was promoted by POFUT2 and B3GLCT-mediated *O*-fucosylation (Holdener and Haltiwanger 2019). This suggests that developmental abnormalities observed in *Pofut2* (Du et al. 2010; Benz et al. 2016) and *B3glct* mouse mutants (Holdener et al. 2019; Neupane et al. 2021) or human Peter's Plus Syndrome (MIM #261540 PTRPLS) patients with inactivating mutations in *B3GLCT* (Hennekam et al. 1993;

Received: October 3, 2022. **Revised:** January 24, 2023. **Accepted:** January 25, 2023

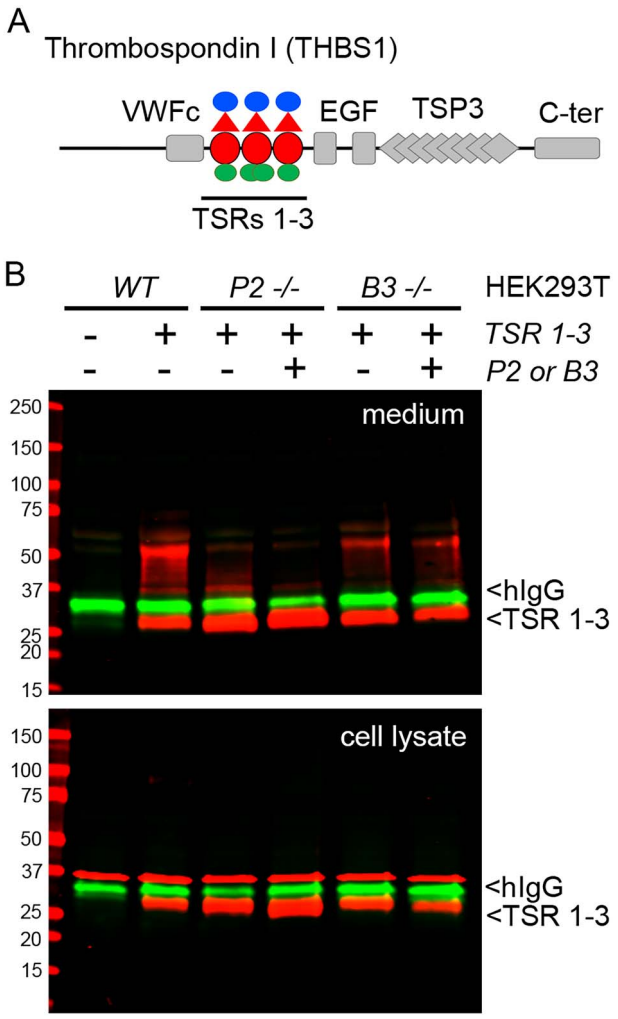

Fig. 1. Secretion of human THBS1 TSRs 1–3 was unaffected by the loss of *POFUT2* or *B3GLCT* in HEK293T cells. (A) Cartoon representation of THBS1 protein domain organization. Domains include von Willebrand factor c-domains (VWFc), thrombospondin type 1 repeats (TSRs; also referred to as TSP1), EGF motifs, thrombospondin type 3 domains (TSP3), and C-terminal domain (C-ter). The location of Myc-tagged TSRs 1–3 construct used for transfections is underlined. Fucose (red triangle), glucose (blue circle), and mannose (green circle) modifications on TSRs 1–3 are shown (Hofsteenge et al. 2001). (B) Representative Western blots from medium (above) and cell lysate (below) of *WT*, *POFUT2*-null (*P2* –/–), or *B3GLCT*-null (*B3* –/–) HEK293T cells that were transfected with expression vector containing Myc-tagged TSRs 1–3 (+) and with (+) or without (–) expression vectors containing *POFUT2 (P2)* or *B3GLCT (B3)*. A construct encoding the Fc portion of heavy chain from human IgG (hIgG) was used as a secretion control with an expected size of ~30 KDa. Blots were probed with anti-Myc and anti-hIgG. The band at ~50 KDa in the medium blot is likely a dimer of THBS1 TSRs 1–3, given it is twice the molecular weight of the expected band. The 37-KDa band in the cell lysates is non-specific as it was detected in negative control (lane 1). Bio Rads Precision Plus Protein™ All Blue Prestained Protein Standards (Cat. No. 1610373) were used for medium and lysate gels.

Hess et al. 2008) result from impaired trafficking of POFUT2/B3GLCT substrates (Holdener and Haltiwanger 2019).

Despite the requirement for the *O*-linked disaccharide for trafficking POFUT2/B3GLCT substrates in cultured HEK293T cells, we recently demonstrated that two POFUT2/B3GLCT substrates, CCN2 and ADAMTS17, were unexpectedly secreted in *Pofut2* conditionally knocked out in developing bone (Neupane et al. 2022). This raises the question of whether developmental abnormalities result from altered function of secreted, unfucosylated POFUT2/B3GLCT substrates. Consistent with this possibility, recent structural and functional studies of the BAI1 protein, with four of five TSRs predicted to be modified by POFUT2, uncovered a role for the *O*-linked fucose in modulating receptor/ligand interactions required for dendritic development and synapse formation (Wang et al. 2022). This is reminiscent of the importance of the *O*-fucose modification added by POFUT1 to NOTCH1 epidermal growth factor-like (EGF) repeats that participate in ligand binding (Luca et al. 2015, 2017).

As THBS1 peptides containing the POFUT2 consensus sequence were reported to alter its interactions with histidine-rich glycoprotein (C^1SVTC^2G), von Willebrand Factor (VWF, C^1SVTC^2G, C^1STSC^2G), and Angiocidin (C^1SVTC^2G) (reviewed in (Resovi et al. 2014), we wanted to determine if the *O*-linked glucose-fucose disaccharide was required for efficient THBS1 trafficking in vivo. As a major source of THBS1 is the secretory granules of tiny anucleate platelets derived from megakaryocytes, we evaluated the THBS1 levels in platelets isolated from *B3glct* knockout and *Pofut2* conditional knockout mice. For conditional knockout experiments, we deleted *Pofut2* in the megakaryocyte precursors of the platelets. We used mass spectral analyses to demonstrate that, in the absence of POFUT2- or B3GLCT-mediated *O*-fucosylation, THBS1 transited to the secretory granules of the platelets and was present at levels comparable to control platelets. The results from these studies showed that although *O*-fucosylation stabilizes TSRs from THBS1, *O*-fucosylation is dispensable for THBS1 trafficking. We also showed that all three TSRs from THBS1 from control and knockout platelets were heavily modified with *C*-mannose even in the absence of *O*-fucose. As *C*-mannose has been shown to stabilize TSRs (Shcherbakova et al. 2019), *C*-mannosylation provides a potential mechanism for trafficking of THBS1 in the absence of *O*-fucosylation. These results raise the possibility that the *O*-fucose modification is having a downstream effect on THBS1 protein–protein interactions and THBS1 cell-signaling in the extracellular environment.

Results

Secretion of THBS1 TSRs 1–3 is unaffected by the loss of POFUT2 and B3GLCT in vitro

All three TSRs of THBS1 have consensus sites for modification by POFUT2 and B3GLCT and are modified at high stoichiometry with the glucose-fucose disaccharide (Fig. 1A) (Hofsteenge et al. 2001). Previous siRNA knockdown of either *POFUT2* or *B3GLCT* in HEK293T cells impaired secretion of THBS1 TSRs 1–3 (Vasudevan et al. 2015). In contrast to these findings, we determined that CRISPR-Cas9 knockout of *POFUT2* or *B3GLCT* in HEK293T cells did not reduce the secretion of THBS1 TSRs 1–3 (Fig. 1B). Overexpression of POFUT2 or B3GLCT in the *POFUT2*-null or *B3GLCT*-null cells, respectively, did not have any significant effects on secretion.

THBS1 levels in platelets are not reduced by the loss of *Pofut2* or *B3glct* in vivo

Due to the opposing CRISPR-Cas9 knockout and siRNA knockdown results in HEK293T cells, we wanted to evaluate

the effects of blocking *O*-fucosylation or extension to the disaccharide on THBS1 trafficking in vivo, in cells specialized to produce and secrete THBS1. To evaluate THBS1 trafficking, we used a combination of Western blot and mass spectral analyses to evaluate the role of the *O*-linked disaccharide on THBS1 levels and glycosylation in platelets isolated from *B3glct* knockout (*B3glct* KO) animals (Holdener et al. 2019) or animals with *Pofut2* conditionally deleted in the megakaryocyte lineage (*Pofut2-PF4* CKO*)* using *PF4-cre* recombinase (Tiedt et al. 2007). The megakaryocyte is a major site of *Thbs1* expression in the embryo and mature animals (Santoro and Frazier 1987; Iruela-Arispe et al. 1993). THBS1 is synthesized as a trimer in the megakaryocyte and is subsequently trafficked through the Golgi and stored in the secretory granules of platelets (Lawler 1986).

Histological evaluation of blood smears from control, *Pofut2-PF4* CKO, and *B3glct* mutants showed platelet morphology comparable to controls (Fig. 2A–D), suggesting that the loss of *Pofut2* or *B3glct* did not grossly impact platelet cell differentiation (Santoro and Frazier 1987; Iruela-Arispe et al. 1993). Using Western blot analyses, we determined that THBS1 was present at comparable levels in platelet cell lysates isolated from control, *Pofut2-PF4* CKO, and *B3glct* knockout mice (Fig. 2E and F). For all genotypes, THBS1 was sensitive to PNGaseF digestion and resistant to EndoH digestion (Supplementary Fig. S1), suggesting that the protein had trafficked through the Golgi to storage granules, and that *O*-linked glucose-fucose disaccharide was not essential for THBS1 trafficking.

To verify the loss or truncation of *O*-linked glycans on TSRs from THBS1 in *Pofut2* or *B3glct* mutants, we performed a glycoproteomic mass spectral analysis of proteins isolated from platelets of control and mutant mice as described in Materials and methods. To detect all three TSR *O*-fucose glycan sites and other THBS1 glycosylation sites of interest, we performed three different types of enzymatic digestions (see Materials and methods). For each TSR in wild-type (*WT*) control mice, the dominant glycoform was the glucose-fucose disaccharide (Fig. 3A–C). The TSR1 and TSR3 peptides were fully modified with the glucose-fucose disaccharide (Fig. 3A and C, Supplementary Figs S2A and D, S4A and E), whereas the TSR2 peptide was modified with ~65 percent glucose-fucose disaccharide and ~ 35 percent fucose monosaccharide (Fig. 3B, Supplementary Fig. S3A, B, and E). No unmodified peptides were detected in any WT control mice. The level of disaccharide and monosaccharide modified peptides in platelets derived from cells with one functional copy of *Pofut2* was similar to that observed in controls for each TSR peptides (Fig. 3A–C). In contrast, the unmodified peptide for each TSR was the major glycoform in platelets from *Pofut2-PF4* CKOs (Fig. 3A–C, Supplementary Figs S2B and E, S3C and E, S4B and E). TSR1 and TSR2 had near-complete loss of *O*-fucose modification, whereas a significant percentage of disaccharide-modified TSR3 peptide was detected (Fig. 3C, Supplementary Fig. S4C). The residual *O*-fucosylation on TSR3 is likely due to incomplete deletion of *Pofut2* by the PF4-driven Cre-recombinase in the megakaryocytes or minor contamination from red blood cells during platelet isolation. In addition, the MS2 fragmentation data for the TSR3 peptide was weakest of the three (Fig. S4), so this may be an incorrect assignment. Nonetheless, we have included these data because it still shows a significant decrease in *O*-fucose.

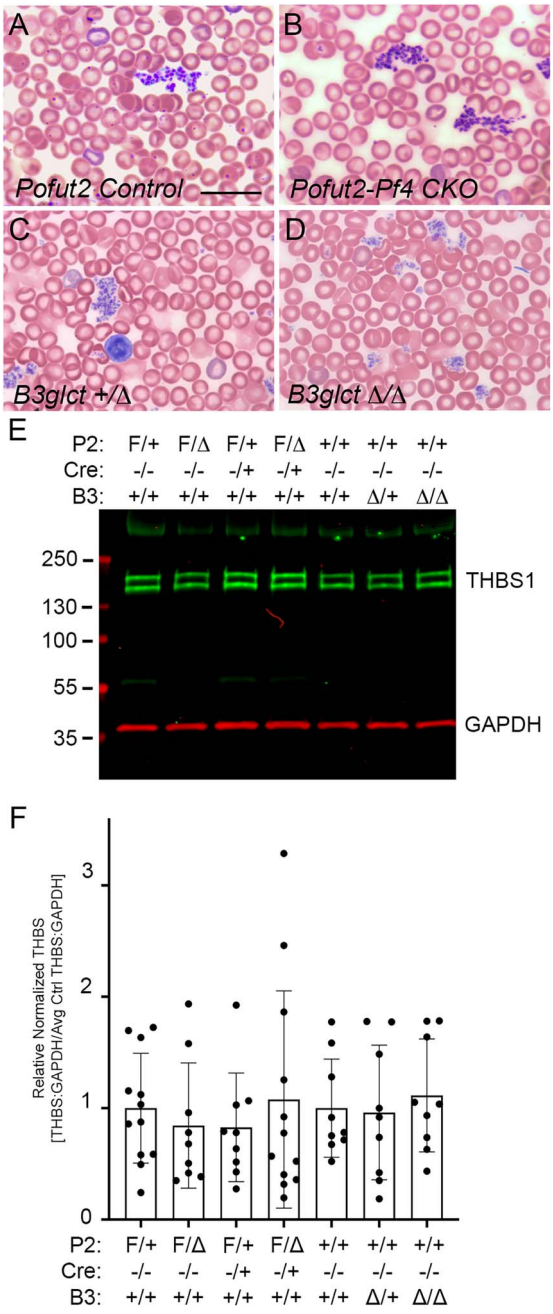

Fig. 2. Thrombospondin 1 levels in platelets are unaffected by the loss of POFUT2 or B3GLCT. (A–D) Representative Wright's stain of whole blood smears from (A) control animals heterozygous for the *Pofut2 floxed* allele and heterozygous for *Pf4-Cre* (*Pofut2 F/+;Pf4+/–)* or (B) *Pofut2-Pf4 CKO* animals that were compound heterzygotes for the *Pofut2-floxed* (F) and *Pofut2* deletion (Δ) alleles and heterozygous for *PF4-cre* (*Pofut2 F/*Δ*;Pf4-cre +/–*), (C) control animals heterozygous for the *B3glct* KO (*B3glct +/*Δ), or (D) homozygous for the *B3glct KO* (*B3glct* Δ*/*Δ*)*. Scale bar in (A) (same for A–D) is 20 μm. (E) Representative Western blot analysis of THBS1 in 4-μg platelet protein extract isolated from animals of indicated genotypes. THBS1 bands of approximately 130 and 160 KDa were consistent with previously reported thrombin-cleaved THBS1 fragments (Lawler et al. 1982, 1985). Molecular weight markers ThermoScientific PageRuler Plus Prestained Protein Ladder (Cat. # PI26619). (F) Quantitation of THBS1 levels of controls relative to *Pofut2-Pf4 CKO* (*P2 F/*Δ*; Pf4-cre –/+; B3 +/+*) or *B3glct KO* (*P2 +/+; Cre –/–; B3* Δ*/*Δ*)* animals (three biological replicates per genotype and three technical replicates per biological sample). Abbreviations: F, floxed; +, WT; Δ, deletion (loxP sites recombined); P2, *Pofut2*; cre, cre-recombinase; B3, *B3glct*).

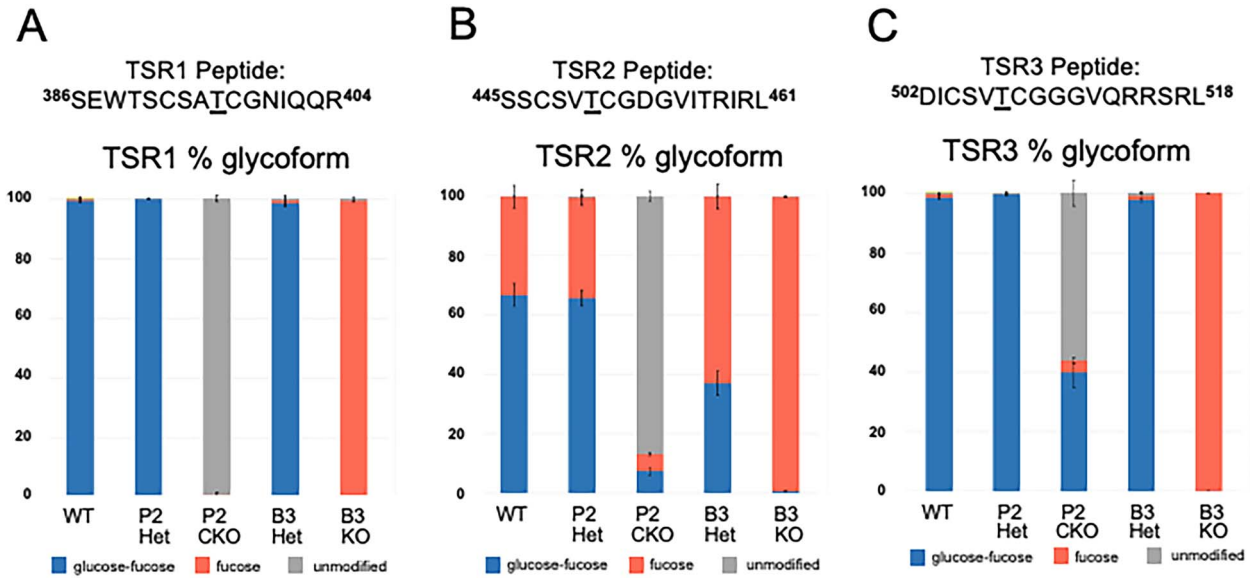

Fig. 3. Significant loss of TSR1–3 *O*-fucosylation on THBS1 from *Pofut2* or *B3glct* knockout platelets. A chymotryptic/tryptic peptide from THBS1 TSR1 (A) and Chymotryptic peptides from THBS1 TSR2 (B) and THBS1 TSR3 (C) were used to determine and quantify different *O*-fucose glycoforms from platelets of WT-control, *Pofut2-Pf4* CKO, and *B3glct* KO mice. Each peptide contains the full consensus sequence for *O*-fucosylation. For each genotype, *O*-fucose peptide glycoforms were quantified and graphed as the total percentage. EICs and MS/MS spectra for ions used are in Supplemental Figs S2–S4. Abbreviations: *Pofut2-Pf4 CKO Het,* P2 Het; *Pofut2-Pf4 CKO,* P2 CKO; *B3glct* +/Δ; B3 Het, *B3glct* Δ / Δ, B3 KO. Biological replicates for all mass spectrometry experiments were $n = 4$ for all *Pofut2* genotypes and $n = 3$ for all *B3glct* genotypes.

In platelets from *B3glct* heterozygotes, the TSR1 and TSR3 peptide were primarily modified with disaccharide similar to controls (Fig. 3A and C, Supplementary Figs S2A and D, S3D and E, S4A and E). In contrast, the TSR2 peptide was primarily modified with monosaccharide, with a significant reduction of the disaccharide glycoform compared with controls (Fig. 3B, Supplementary Fig. S3B and E). In platelets from *B3glct* knockout mice all three TSRs were modified with the fucose monosaccharide glycoform only, consistent with the complete loss of B3GLCT activity (Fig. 3A–C, Supplementary Figs S2C and D, S3D and E, S4D and E). These results confirm the loss of POFUT2 and B3GLCT function in the *Pofut2-PF4* CKO mice and *B3glct* KO mice, respectively.

We also queried our mass spectral dataset to determine whether THBS1 *N*-glycans were oligomannose, hybrid, or complex. If THBS1 was unable to transit through the Golgi apparatus due to the loss of *O*-fucose, THBS1 would be trapped in the ER, preventing processing of its four predicted *N*-glycans to complex or hybrid forms. We were able to detect a THBS1 peptide containing an *N*-glycan site that was modified with multiple hybrid or complex type *N*-glycans (Fig. 4A). In all mice, the hybrid or complex type *N*-glycan was the predominant species indicating that THBS1 had trafficked through the Golgi apparatus in the absence of POFUT2 or B3GLCT modifications (Fig. 4A, Supplementary Fig. S5A–F). No oligomannose species were detected. Furthermore, quantitation of each glycoform from all genotypes was strikingly similar (Fig. 4A, Supplementary Fig. S5F), indicating that the neither the disaccharide nor unmodified forms of the TSR3 peptide from *Pofut2-PF4* CKO mice (Fig. 3C) affected trafficking and secretion of THBS1. Additionally, another peptide with an *N*-glycan site from THBS1 was detected in all samples, and all glycoforms of that peptide were of the complex type in all mice genotypes (Tables SI–SXVIII). Finally, comparison of the level of THBS1 to that of another highly abundant protein in platelet granules in our proteomics data, vWF, showed that the level THBS1 from *Pofut2-PF4* CKO or *B3glct* KO mice was similar to WT (Fig. 4B, Tables SXIX–SXX), consistent with the Western blotting data in Fig. 2.

C-mannosylation of THBS1 TSRs 1–3 is highly abundant in platelets lacking POFUT2 or B3GLCT

As we observed that *O*-fucosylation of THBS1 was not essential for secretion, we hypothesized that *C*-mannosylation of TSRs from THBS1 is sufficient for proper folding and secretion in the absence of *O*-fucosylation. *C*-mannosylation was recently shown to promote folding of *C. elegans* UNC-5 TSR2 as well as stabilize the UNC-5 TSR2 fold (Shcherbakova et al. 2019). Each of the THBS1 TSRs have three tryptophan consensus sites for *C*-mannosylation (WXXWXXWXXC), several of which are known to be modified in THBS1 isolated from human platelets (Hofsteenge et al. 2001). We confirmed that all three TSRs from THBS1 were modified with C-mannose in WT mice (Fig. 5A–C). Peptides from TSR1 and TSR3 were modified with a single *C*-mannose at high stoichiometries (Fig. 5A and C, Supplemental Figs S6A and S8A). A shorter peptide for both TSR1 and TSR3 lacking the third tryptophan in the *C*-mannose consensus sequence was detected and unmodified with mannose (Tables SII–SXVIII), indicating that TSR1 and TSR3 were not fully modified with *C*-mannose. The TSR2 from WT mice was heavily modified with *C*-mannose on two tryptophan residues at the same position as in human THBS1 (Fig. 5B, Supplemental Fig. S7A). Similar results were obtained from *Pofut2* CKO and *B3glct* KO samples, indicating that the loss of *O*-fucose mono- or disaccharide does not affect *C*-mannosylation (Fig. 5A–C, Supplemental Figs S6B–C, S7B–C, S8B–C).

Discussion

Although previous siRNA knockdown studies in HEK293T cells suggested that efficient secretion of THBS1 TSRs

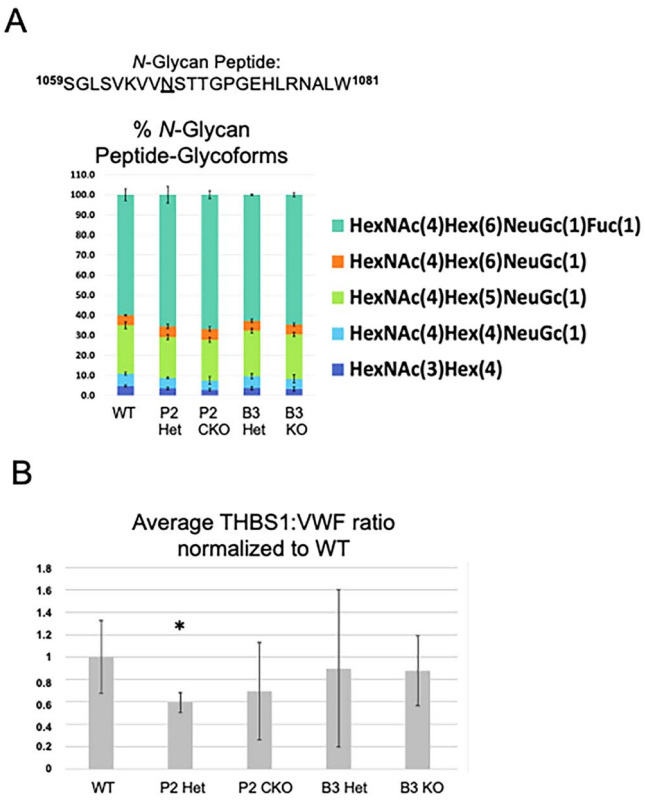

Fig. 4. Thrombospondin 1 levels and trafficking is unaffected by the loss of *Pofut2* and *B3glct* in platelets. (A) A chymotryptic peptide from THBS1 containing an *N*-glycan site was used to determine and quantify different glycoforms of complex and hybrid type *N*-glycans on the peptide from all mouse genotypes. For each genotype, *N*-glycan glycoforms were quantified and graphed as the total percentage. EICs and MS/MS spectra for ions used are in Supplemental Fig. S5. (B) The average ratio of THBS1 to VWF protein (a highly abundant protein found in platelets) peptides in platelet lysates was compared in all mice genotypes. Average ratios in *Pofut2* and *B3glct* mutant platelets were similar to controls. Data were evaluated for statistical significance using unpaired, two-tailed *t*-test. $*P \leq 0.05$, $**P \leq 0.01$, ns, not significant. $P \leq 0.05$. Abbreviations: *Pofut2-Pf4 CKO Het,* P2 Het; *Pofut2-Pf4 CKO,* P2 CKO; *B3glct* +/Δ; B3 Het, *B3glct* Δ/Δ, B3 KO. Biological replicates for all mass spectrometry experiments were $n = 4$ for all *Pofut2* genotypes and $n = 3$ for all *B3glct* genotypes.

1–3 required *O*-fucosylation and extension to the glucose-fucose disaccharide, here we demonstrated that secretion of THBS1 TSRs 1–3 was not reduced in CRISPR-Cas9 knockout of *POFUT2* or *B3GLCT* in HEK293T cells. Furthermore, THBS1 secretion was not detectably reduced in platelets derived from *Pofut2-PF4-Cre* CKO or *B3glct* KO mice. These results are consistent with the recent findings that ADAMTS17 and CCN2 were efficiently secreted in *Pofut2* mutant developing bone (Neupane et al. 2022). A major explanation for the differences observed in siRNA knockdown and CRISPR-Cas9 knockout studies is the potential off-target effects during siRNA knockdown experiments. siRNA knockdown can be promiscuous and can target multiple non-specific gene targets by overloading the RNAi silencing complex (RISC) and associated pathways (Sigoillot and King 2011). Conversely CRISPR-Cas9 knockdown is much more specific to its intended target gene leading to less off-target effects (Boettcher and McManus 2015). These same differences of effects in siRNA knockdown versus CRISPR-Cas9 knockout were previously observed in our lab under similar conditions (Zhang et al. 2020).

These observations raise the possibility that the negative impact of *Pofut2* or *B3glct/B3GLCT* mutations on development stems not only from a potential impact of POFUT2/B3GLCT substrate on folding efficiency and trafficking but also from altered function of secreted TSR-containing proteins lacking the *O*-linked glycan. This conclusion is supported by the recent observation that *O*-linked disaccharide was shown to play a critical role in dendritic development and synapse formation by modulating the interaction between the POFUT2/B3GLCT substrate Brain angiogenic inhibitor (BAI1), an adhesion-G protein coupled receptor (adhesion-GPCR), with its high-affinity ligand, the reticulon-4 receptor (RTN4R, also known as the "NoGo receptor") (Wang et al. 2022). It is also reminiscent of the role of POFUT1-mediated addition of *O*-fucose on EGF Repeats on the Notch receptor, where *O*-fucose modification is important for trafficking of Notch in some cells but not others, but also functions in Notch–ligand interactions (Holdener and Haltiwanger 2019).

C-mannosylation has been observed to be important for the folding and secretion of human ADMATS16 and THBS1 (Cirksena et al. 2021) as well as proteins involved in the transmission of malaria to humans (Albuquerque-Wendt et al. 2020). *O*-fucosylation on the other hand has been shown here and elsewhere (Sanz et al. 2019; Neupane et al. 2022) to be dispensable for folding and secretion in some instances. Importantly, in proteins with *O*-fucosylation but without *C*-mannosylation, such as ADAMTS9 TSR2–8 and ADAMTS20 TSR2–8, secretion is significantly reduced from *POFUT2*-KO HEK293T cells (Holdener et al. 2019). This implies that *O*-fucosylated TSRs that are also *C*-mannosylated may provide other cellular roles besides TSR folding, stability, and secretion. In these cases, *C*-mannosylation may be the driving force for folding and secretion. Therefore, *O*-fucosylation might play a role in downstream protein–protein interactions or cell signaling events in the extracellular environment. Conversely, *O*-fucosylation may simply perform a stabilizing role of TSRs after trafficking through the ER and Golgi by protecting the disulfide bond integrity of the C2-C6 disulfide bond (Berardinelli et al. 2022).

The question of whether the *O*-linked disaccharide modulates THBS1 function is relevant considering that peptides containing the consensus site for *O*-fucosylation (C^1SVTC^2G or C^1STSC^2G) promote adhesion of a number of cell types and inhibit platelet aggregation and tumor cell metastasis (Tuszynski et al. 1992). Consequently, the role of *O*-fucosylation beyond protein folding and secretion has yet to be fully elucidated, and the results provided here and elsewhere (Wang et al. 2022) suggest that the rare *O*-fucose modification may have unique and diverse protein–protein or cell–signaling interactions.

Materials and methods

Ethics statement

All animal work was conducted according to relevant national and international guidelines and under approved protocols. Stony Brook University animal facilities were approved by the NIH Office of Laboratory Animal Welfare, assurance number D-16-00006. The animal studies were approved by

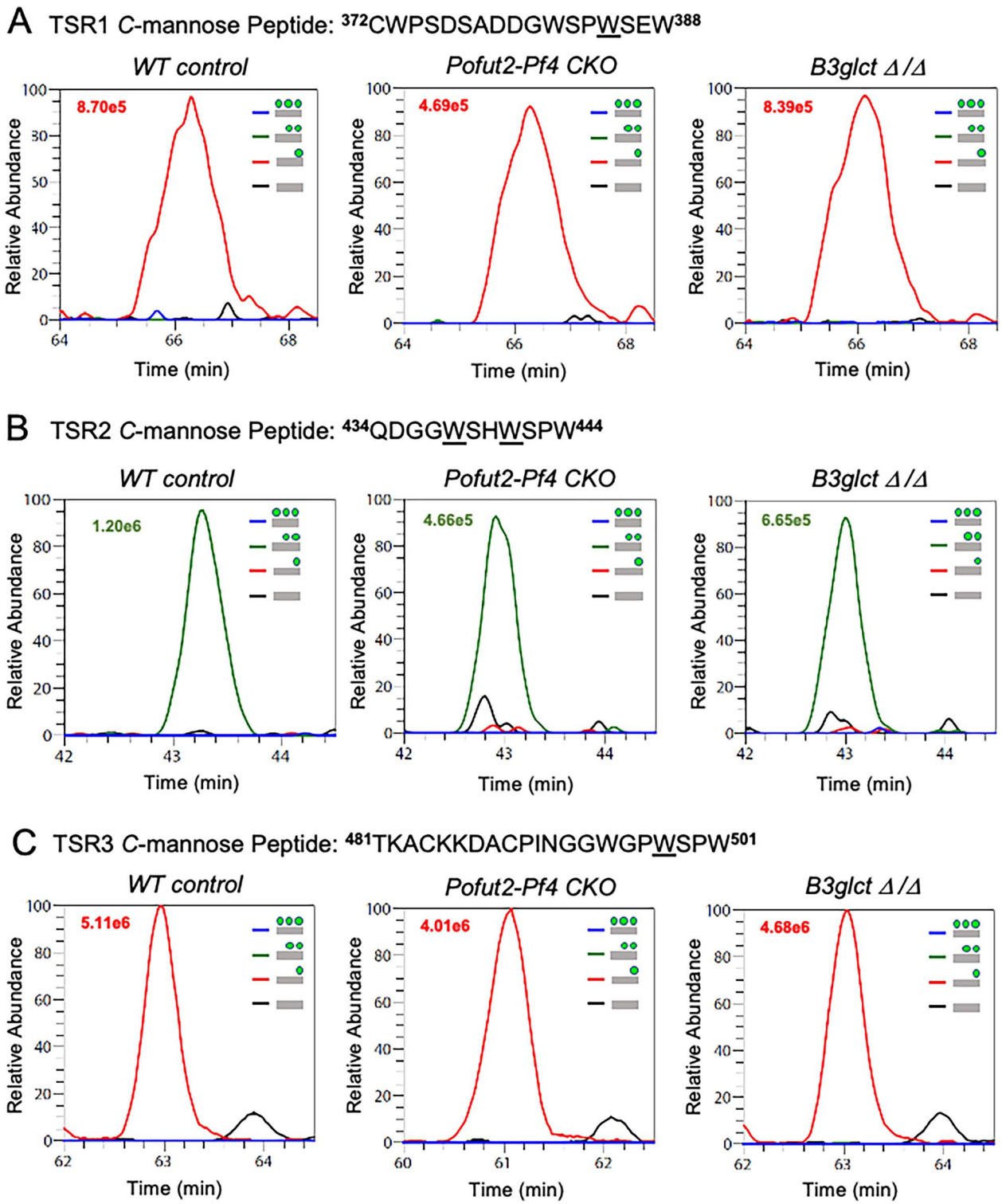

Fig. 5. Thrombospondin 1 TSRs 1–3 from *Pofut2* and *B3glct* knockout mice are *C*-mannosylated in platelets. A chymotryptic/tryptic peptide from THBS1 TSR1 (A), chymotryptic/tryptic peptide from THBS1 TSR2 (B), and chymotryptic/Glu-C peptide from THBS1 TSR3 (C) were used to determine and quantify different *C*-mannose glycoforms from platelets of WT-control, *Pofut2-Pf4* CKO, and *B3glct* KO mice. Each peptide contains the full consensus sequence for *C*-mannosylation. EICs for all mice genotypes show that TSR1 was modified with mannose on the second tryptophan (A), TSR2 was modified with mannose on both the first and second tryptophans (B), and TSR3 was modified with mannose on the second tryptophan in the peptide (C). Ion intensity values of the most abundant ion are shown in the top left corner of each EIC in Fig. 5. MS/MS spectra for ions used are provided in Supplemental Figs S6–S8.

the Stony Brook University Institutional Animal Care and Use Committee, which follows all the guidance set forth in the following: Public Health Service Policy on Humane Care and Use of Laboratory Animals distributed by Office of Laboratory Animal Welfare, NIH; Animal Welfare Act and Animal Welfare Regulations distributed by United States Department of Agriculture and Guide for the Care and Use of Laboratory Animals distributed by the National Research Council. Stony Brook University animal facilities are accredited by AAALAC International (Association for the Assessment and Accreditation of Laboratory Animal Care International).

Mice

All mice were housed and maintained under controlled temperature and light (22°C, 12-hour light and 12-hour dark) with access to food and water. For analyses of *B3glct* knockout effects, diet was supplemented with DietGel® 76A (ClearH20; Cat# 72-07-5022) to ensure that mutants received adequate hydration and nutrition. *Pofut2*$^{tm2.2bch}$ (abbreviated *Pofut2*-Δ) (Benz et al. 2016) and *B3glct*$^{tm1.3Nari}$ (abbreviated *B3glct*-Δ) (Holdener et al. 2019) knockout alleles were maintained by backcrossing to C57BL/6 J. Following extensive backcrossing to C57BL/6 J, the *Pofut2* floxed allele, *Pofut2*$^{tm2.1bch}$ (*Pofut2-floxed*) (Benz et al. 2016) was maintained by intercrossing homozygotes, with backcross to C57BL/6 J at least every fifth generation to prevent genetic drift. For conditional knockout of *Pofut2* in platelets, we utilized codon optimized cre-recombinase strain C57BL/6-Tg(*Pf4*-icre)Q3Rsko/J (Jax Stock# 008535) (*Pf4-icre,* also known as *Cxcl4-iCre*) (Tiedt et al. 2007) obtained from The Jackson Laboratory (Bar Harbor, ME). Conditions used for genotyping *Pofut2* and *B3glct* animals was as previously described (Neupane et al. 2021, 2022) and *Pf4-icre* genotyping strategies are described in The Jackson Laboratory Genotyping Protocol Database: https://www.jax.org/jax-mice-and-services/customer-support/technical-support/genotyping-resources/genotyping-protocol-database.

Cell-based secretion assays and Western blots of human THBS1 TSRs 1–3

A plasmid encoding human THBS1 TSRs 1–3 in pSecTag2C backbone vector (Vasudevan et al. 2015) was transfected into WT HEK293T cells, *POFUT2* KO (Benz et al. 2016), and *B3GLCT* KO (Hubmacher et al. 2017) HEK293T cells. A total of 1.94 μg of plasmids was transfected into each cell line using polyethylimine as a transfection reagent (Thomas et al. 2005) at a ratio of 6 μl of PEI per 1 μg of plasmid transfected. WT cells were transfected with 1.74 μg of pSecTag2C empty vector and 0.2 μg of a plasmid encoding the Fc portion of human IgG (hIgG-pRK5) (Wang et al. 2007; Vasudevan et al. 2015) or 1.5 μg of THBS1 TSRs 1–3, 0.24 μg of pSecTag2C empty vector, and 0.2 μg of hIgG-pRK5. *POFUT2* KO cells were transfected with 1.5 μg of THBS1 TSRs 1–3, 0.24 μg of pSecTag2C empty vector or pCDNA4-POFUT2 (Benz et al. 2016) and 0.2 μg of hIgG-pRK5. *B3GLCT* KO cells were transfected with 1.5 μg of THBS1 TSRs 1–3, 0.24 μg of pSecTag2C empty vector or pCDNA3.1-B3GLCT (Sato et al. 2006) and 0.2 μg of hIgG-pRK5. The hIgG plasmid was used as a loading and secretion control while the POFUT2 and B3GLCT plasmids were used for rescue of secretion in the *POFUT2* KO and *B3GLCT* KO cell lines, respectively. Samples were transiently transfected in OPTI-MEM (vendor) which included plasmids and PEI. After 48 hours post-transfection, media samples were collected and cells were lysed in a buffer containing 1 percent Triton-X 100, 25-mM Tris, pH 8.0 containing a cOmplete™ protease inhibitor cocktail tablet (Roche, Cat. No. 11836145001).

Western blots were run on a 4–20 percent gradient gel (Bio-Rad) and transferred to a nitrocellulose membrane and incubated in anti-Myc (9E10, Stony Brook University Cell Culture/Hybridoma facility) at a 1:2,000 ratio for TSRs 1–3 detection and incubated overnight at 4°C. Membranes were then washed in TBST, incubated in Alexa Fluor IRDye® 680RD goat anti-mouse (LI-COR, Cat. No. 926-68070) for THBS1 TSRs 1–3 detection and IRDye® 800CW goat (polyclonal) anti-human IgG (H 1 L) (LI-COR catalog number 925-32232) for hIgG detection. Both secondary antibodies were used at a 1:10,000 ratio for 1 hour at room temperature in the dark. Membranes were then scanned and imaged on an Odyssey CLx instrument (LI-COR Biosciences).

Animal crosses for analysis of THBS1 in platelets

For analyses of the effects of loss of POFUT2 on thrombospondin in platelets, we crossed congenic (N15) females heterozygous for the *Pofut2*-Δ knockout allele (*Pofut2*-Δ/+) to males hemizygous for the *Pf4-icre* allele to generate *Pofut2*-Δ/+;*Pf4-icre hemizygous* (N1) males. *Pofut2*-Δ/+; Pf4-icre *hemizygous* males were mated to females homozygous for the *Pofut2* floxed allele (*Pofut2-Floxed/Floxed*) to generate *Pofut2-Flox*/+;Pf4-icre negative, *Pofut2-Flox*/Δ;Pf4-icre negative, *Pofut2-Flox*/+;Pf4-icre *hemizygous,* and *Pofut2-Flox*/Δ;Pf4-icre *hemizygous* animals used for the study. For analyses of the effects of the loss of B3GLCT on thrombospondin in platelets, we intercrossed congenic (N13) animals heterozygous for the *B3glct* knockout allele (*B3glct*-Δ/+) to generate *B3glct* − +/+ (control), *B3glct*-Δ/+, and *B3glct*-Δ/Δ animals.

Platelet collection and Western blot analyses

Platelets were isolated from whole blood as previously described with some modifications (Im and Muschel 2017; Aurbach et al. 2019). Briefly, total blood was collected from anesthetized mice 2–5 months of age by cardiac puncture into the 150-μl acid-citrate-dextrose buffer and mixed by inversion. Platelet washing buffer was added to the collected blood, and the sample was centrifuged at 180 rcf for 8 minutes. The upper platelet rich plasma was transferred to a new tube. The lower red blood cell layer was washed with platelet washing buffer, centrifuged as before, and the upper platelet-rich plasma layer was removed and combined with the first collection. Platelets were pelleted by centrifugation at 1,250 rcf at 22°C for 10 minutes, and platelets were gently re-suspended in the 1-ml platelet washing buffer and pelleted as above. The supernatant was removed and the platelet pellets were flash frozen in liquid nitrogen prior to storage at −80°C and tissue lysis for subsequent Western and mass spectral analyses. Each platelet pellet was lysed in the 125-μl RIPA Buffer (ThermoScientific, Cat # PI89900) containing 1 X EDTA-free, protease inhibitor (Genesse, Cat # 18-420) for 90 minutes on ice with periodic pipetting and vortexing. Samples were then centrifuged at 13,800 rcf and 4°C for 15 minutes and the supernatants collected. The protein concentration was determined by BCA Protein Assay kit (Pierce, Cat # 23227) as per the manufacture's microplate procedure.

For Western blot analysis of THBS1, 4 μg of platelet protein lysate in 2 X Laemmli sample buffer with 0.2-M DTT (for reducing gels) was separated on 4–15 percent gradient acrylamide gels (BioRad, Cat # 4561083), and transferred to nitrocellulose membranes. For thw detection of THBS1 on Western blots, nitrocellulose membranes were simultaneously probed with a 1:1,000 dilution of primary Monoclonal Mouse anti-Thrombospondin 1 (A6.1) (Santa Cruz Biotechnology Inc. Cat #sc-59,887; RRID: AB_793045) and a 1:20,000 dilution of polyclonal rabbit anti-GAPDH (Sigma Cat #G9545; RRID: AB_796208) and incubated overnight at 4°C. After washing with TBST, membranes were simultaneously probed with secondary antibodies including IRDye® 800CW Goat anti-Mouse IgG (LICOR Cat #925–32,210; RRID: AB2687825) and IRDye® 680RD Goat anti-Rabbit IgG (LICOR Cat #925–68,071; RRID: AB_2721181) at dilutions of 1:12,500 and 1:25,000, respectively. Membranes were allowed to incubate for 1 hour at room temperature. After probing, membranes were imaged using Odyssey CLx, Model 9140 and data were evaluated using Image Studio Ver. 5.2 and Empiria Studio 2.1 from LI-COR. All fluorescence signals were within the linear range of detection and were normalized to GAPDH and plotted relative to the average of the control animals. Three animals for each genotype were used with three technical replicate Western blots performed for each animal. Statistical analyses of relative normalized fluorescent signals were performed using GraphPad prism software (Version 8) to evaluate significance using unpaired, two-tailed *t*-test with $P < 0.05$ considered significant.

Blood smear preparation and wright stain

For histological evaluation of blood, monolayer of peripheral blood smear was prepared from a small drop of blood collected from lateral tail vein and air-dried as described previously (Houwen 2002) The blood smears were then stained with Wright stain (Harleco® Wright Stain Solution, Cat # 740-75, EMD Millipore) by dip slide method according to manufacturer's instructions. Briefly, air dried slides were fixed in methanol for 30 seconds, kept slides in Wright stain for 3 minutes, placed slides in the freshly prepared Stain-Buffer Mixture for 6 minutes, rinsed with 15 ml of deionized water and air-dried. Then slides were mounted with mounting media and cover slipped. The blood smear was photographed at 100 X using a Nikon Optiphot microscope, AxioCam MRc camera and AxioVisionLE program (Zeiss).

Mass spectrometry sample preparation and parameters used for data acquisition

Platelets from all genotypes were isolated as described above and lysed in RIPA buffer containing a 1 X EDTA-free PIC tablet (Roche, Cat # 1187358001) by sonicating for two 1-second pulses, rotated at 4°C for 20 minutes, and clarified by centrifugation for 10 minutes, max speed at 4°C. Quantification of lysates was determined by BCA assay (Pierce, Cat # 23227). Roughly 10 μg of protein from each sample was denatured and reduced for 5 minutes at 50°C in a buffer consisting of 8-M urea, 400-mM ammonium bicarbonate, and 10-mM TCEP, then alkylated using 100-mM iodoacetamide for 30 minutes at room temperature in the dark. Samples were then diluted to 2-M urea and digested with 500-ng chymotrypsin (Thermo Fisher, Cat # 90056) or 250 ng of chymotrypsin plus 250 ng of trypsin (Thermo Fisher, Cat # 90058) or 250 ng of chymotrypsin plus 250 ng of Glu-C (Sigma Aldrich, Cat # P2922-100UN) for 4 hours at 37°C. Subsequently, samples were then acidified with 5 percent formic acid, sonicated for 20 minutes, then desalted with a C18 ZipTip (Millipore, Cat # ZTC18S960).

Samples were then injected onto a Q-Exactive Plus Orbitrap mass spectrometer (Thermo Fisher Scientific) equipped with an EASY-nanoLC 1000 (Thermo Fisher Scientific) and a EasySpray PepMap RSLC C18 column (50 μm × 15 cm; Thermo Fisher) for peptide separation. Peptides were separated using a linear 90-minute binary gradient consisting of solvent A (5 percent acetonitrile in 0.1 percent formic acid) and solvent B (80 percent acetonitrile in 0.1 percent formic acid) at a 300 nl/min constant flow rate. Data dependent acquisition of spectra was performed with a resolution of 70,000 over an m/z range of 400–2,000 m/z in the positive polarity mode with a targeted automatic gain control of 1×10^6. The 10 most abundant precursor ions in full MS scans were isolated and subjected to MS/MS fragmentation by higher energy collisional dissociation-tandem mass spectrometry (HCD-MS/MS) using a normalized collision energy of 27 percent, with a targeted automatic gain control of 1×10^5, in addition to a 1.2 m/z isolation window. Dynamic exclusion was enabled along with a fragment resolution of 17,500.

Detection and quantification of glycopeptides and THBS1

Detection of all *O*-fucose and *C*-mannose peptides was performed using Byonic software version 2.10.5 (Protein Metrics) as a node in Proteome Discoverer software version 2.1.0.81 (Thermo Fisher) using a whole mouse database (Uniprot Proteome Identifier: UP000000589). Fixed modifications: carbamidomethyl +57.021464 at C. Variable modifications: oxidation +15.994915 at D, H, N, and deamidated +0.984016 at N. Variable glycan modifications: Fuc(1) at S, T, Hex(1)Fuc(1) at S,T, and Hex(1) at W. Precursor and fragment mass tolerances was set to 20 and 30 ppm, respectively. Three missed cleavages were allowed for all three digestion datasets except for the chymotrysin/glu-c dataset, as our peptide of interest (C-mannose from TSR3) had four missed cleavages. Protein and peptide false discovery rates were set to a threshold of 1 percent and calculated using the two-dimensional (2D FDR) target/decoy strategy as described (Bern and Kil 2011) and were then further filtered to have a Byonic score greater than 100 and a PEP value lower than 1×10^{-3}. MS/MS spectra used for quantification were manually examined. Quantification of *O*-fucose and *C*-mannose peptides was determined using Xcalibur™ software version 4.0.27.19 (Thermo Fisher Scientific) by taking area under the curve (AUC) of extracted ion chromatograms (EICs). Lists of all peptides and PSMs found containing the consensus sequences (partial and full consensus sequences) for *O*-fucose and *C*-mannose that were used for quantitation and generating EICs in Figs 3A–B, 5A–C, S2D and E, S4E from each .raw file can be found in Supplementary Tables SI–SXVIII. Due to the lability of the fucose-peptide bond in high energy collision dissociation experiments, Byonic is frequently unable to correctly assign the *O*-fucosylated Ser/Thr residue in a peptide. All assignments are based on the well documented sequence for *O*-fucosylation of Group 1 TSRs: $C^1XX(S/T)C^2$. In contrast, the *C*-mannose peptide bond is stable, so *C*-mannosylated tryptophans can be identified in MS/MS spectra. It is unlikely that a peptide with a *C*-mannosylated tryptophan can be cleaved by chymotrypsin.

Detection of the THBS1 *N*-glycan peptide glycoforms was performed using Byonic standalone software version 4.1.10 (Protein Metrics) and was searched against a whole mouse database (Uniprot Proteome Identifier: UP000000589). *N*-glycan modifications were searched against a Byonic library consisting of 309 different mammalian *N*-glycan glycoforms. No fixed or variable modifications were used except for *N*-glycan modification at N. Precursor and fragment mass tolerances was set to 10 and 20 ppm, respectively, with three missed cleavages allowed. Protein and peptide false discovery rates were set to a threshold of 1 percent and calculated using the 2-dimensional (2D FDR) target/decoy strategy as described (Bern and Kil 2011) and were then further filtered to have a Byonic score greater than 100 and a PEP value lower than 1×10^{-3}. Spectra generated in Byonic was used for each *N*-glycan glycoform for Fig. S5(A–E) to observe sugar oxonium ions in addition to b- and y-ions. MS/MS spectra for *N*-glycosylated peptides used for quantification were manually annotated. Quantitation for top 5 most abundant *N*-glycan glycoforms detected was performed by generating EICs using Xcalibur Qual Browser software version 2.0.3.2 (Thermo Fisher) and taking area under the curve. All other *N*-glycan glycoforms not quantified were of the complex or hybrid type and no high mannose glycoforms were detected. Lists of all peptides and PSMs found containing the *N*-glycan site that was used for quantitation and generating EICs in Figs 4(A) and S5(F) from each .raw file can be found in Tables SI–SXVIII.

For the comparison of THBS1 to vWF, raw files were processed through Proteome Discoverer version 2.5.0.400 (Thermo Fisher) to identify and quantify peptides. Default processing and consensus workflows provided by Proteome Discover were used for precursor ion quantitation. To determine protein abundances, the TopN approach was used in which the top 5 most abundant peaks/peptides from each protein were averaged and used for quantitation of each protein. Filters were set to a 1 percent false discovery rate and minimum peptide length of six amino acids and samples were searched against a whole mouse database (Uniprot Proteome Identifier: UP000000589). The generated data were exported to an Excel file by Proteome Discoverer in which the total protein abundance for each sample was calculated by summarizing the top 50 protein abundances detected and can be found in Tables SXIX–SXX. Samples were then normalized to the sample with the highest protein abundance which was then used to determine the average abundance for all proteins. Fold changes between THBS1 and vWF in each genotype were then calculated by dividing the knockout average of THBS1 by the control/WT average of vWF. Statistical significance was determined by performing a two-tailed *t*-test.

Acknowledgements

The authors would like to acknowledge all the Holdener and Haltiwanger lab members for their positive critiques while discussing this paper during lab meeting.

Author contributions

S.J.B., A.R.S, R.C.G., R.S.H. and B.C.H.: conceptualization; R.S.H and B.C.H.: funding acquisition, project administration and supervision; S.J.B., A.R.S., R.C.G., S.N., A.I., R.S.H. and B.C.H.: investigation; S.J.B. and B.C.H.: writing original draft; S.J.B., A.R.S., R.C.G., S.N., A.I., R.S.H. and B.C.H.: writing, reviewing and editing.

Supplementary material

Supplementary material is available at *GLYCOB Journal* online.

Funding and additional information

This work was supported by grants provided by the National Institute of Health (HD096030 and HD090156 to R.S.H. and B.C.H.)

Conflict of interest statement. None declared.

Data availability

The mass spectrometry proteomics data have been deposited to the ProteomeXchange Consortium via the PRIDE (Perez-Riverol et al. 2019) partner repository with the data set identifier PXD037158.

Abbreviations and nomenclature

ADAMTS17, A Disintegrin and Metalloproteinase with Thrombospondin motifs 17; BAI1, Brain-specific angiogenesis inhibitor 1; B3GLCT, b1,3 glucosyltransferase; BCA Bicinchoninic acid; CRISPR, clustered regularly interspaced short palindromic repeats; Cas9, Crisper associated protein 9; CCN2, Cellular Communication Network Factor 2; CD36, Cluster of differentiation 36; Cys, Cysteine; DTT, Dithiothreitol; EDTA, Ethylenediaminetetraacetic acid; EGF, Epidermal growth factor; ECM, Extracellular matrix; GAPDH, Glyceraldehyde-3-phosphate dehydrogenase; GPCR, G protein coupled receptor; HPLC, High performance liquid chromatography; hIgG, Human immunoglobulin G; PIC, Netrin receptor c; Protease inhibitor cocktail; POFUT1, Protein O-fucosyltransferase 1; POFUT2, Protein O-fucosyltransferase 2; siRNA, small interfering ribonucleic acid; RISC, RIPA buffer, Radioimmunoprecipitation assay buffer; RNA-induced silencing complex; RTN4R, reticulon-4 receptor; TBST, Tris Buffered saline containing Triton-x100; TCEP, (tris(2-carboxyethyl)phosphine); TGFβ, Transforming growth factor beta; THBS1, Thrombospondin 1; TSP1, Thrombin sensitive protein 1; TSR, Thrombospondin Type 1 Repeat; UNC-5, VEGFA, Vascular Endothelial Growth Factor A; vWF, von Willebrand factor.

References

Albuquerque-Wendt A, Jacot D, dos Santos Pacheco N, Seegers C, Zarnovican P, Buettner FFR, Bakker H, Soldati-Favre D, Routier FH. C-mannosylation of toxoplasma gondii proteins promotes attachment to host cells and parasite virulence. *J Biol Chem*. 2020:**295**(4):1066–1076.

Aurbach K, Spindler M, Haining EJ, Bender M, Pleines I. Blood collection, platelet isolation and measurement of platelet count and size in mice-a practical guide. *Platelets*. 2019:**30**(6):698–707.

Baenziger NL, Brodie GN, Majerus PW. A thrombin-sensitive protein of human platelet membranes. *Proc Natl Acad Sci USA*. 1971:**68**(1):240–243.

Benz BA, Nandadasa S, Takeuchi M, Grady RC, Takeuchi H, LoPilato RK, Kakuda S, Somerville RPT, Apte SS, Haltiwanger RS, et al. Genetic and biochemical evidence that gastrulation defects in Pofut2 mutants result from defects in ADAMTS9 secretion. *Dev Biol*. 2016:**416**(1):111–122.

Berardinelli SJ, Eletsky A, Valero-Gonzalez J, Ito A, Manjunath R, Hurtado-Guerrero R, Prestegard JH, Woods RJ, Haltiwanger RS. O-fucosylation stabilizes the TSR3 motif in thrombospondin-1 by interacting with nearby amino acids and protecting a disulfide bond. *J Biol Chem*. 2022:**298**(6):102047.

Bern MW, Kil YJ. Two-dimensional target decoy strategy for shotgun proteomics. *J Proteome Res*. 2011:**10**(12):5296–5301.

Boettcher M, McManus MT. Choosing the right tool for the job: RNAi, TALEN, or CRISPR. *Mol Cell*. 2015:**58**(4):575–585.

Cirksena K, Hütte HJ, Shcherbakova A, Thumberger T, Sakson R, Weiss S, Jensen LR, Friedrich A, Todt D, Kuss AW, et al. The C-mannosylome of human induced pluripotent stem cells implies a role for ADAMTS16 C-Mannosylation in eye development. *Mol Cell Proteomics*. 2021:**20**:100092.

Du J, Takeuchi H, Leonhard-Melief C, Shroyer KR, Dlugosz M, Haltiwanger RS, Holdener BC. O-fucosylation of thrombospondin type 1 repeats restricts epithelial to mesenchymal transition (EMT) and maintains epiblast pluripotency during mouse gastrulation. *Dev Biol*. 2010:**346**(1):25–38.

Dubail J, Vasudevan D, Wang LW, Earp SE, Jenkins MW, Haltiwanger RS, Apte SS. Impaired ADAMTS9 secretion: A potential mechanism for eye defects in Peters Plus Syndrome. *Sci Rep*. 2016:**6**(1):33974.

Hennekam RC, Van Schooneveld MJ, Ardinger HH, Van Den Boogaard MJ, Friedburg D, Rudnik-Schoneborn S, Seguin JH, Weatherstone KB, Wittebol-Post D, Meinecke P. The Peters'-Plus syndrome: description of 16 patients and review of the literature. *Clin Dysmorphol*. 1993:**2**(4):283–300.

Hess D, Keusch JJ, Oberstein SA, Hennekam RC, Hofsteenge J. Peters plus syndrome is a new congenital disorder of glycosylation and involves defective O-glycosylation of thrombospondin type 1 repeats. *J Biol Chem*. 2008:**283**(12):7354–7360.

Hofsteenge J, Huwiler KG, Macek B, Hess D, Lawler J, Mosher DF, Peter-Katalinic J. C-mannosylation and O-fucosylation of the thrombospondin type 1 module. *J Biol Chem*. 2001:**276**(9):6485–6498.

Holdener BC, Haltiwanger RS. Protein O-fucosylation: structure and function. *Curr Opin Struct Biol*. 2019:**56**:78–86.

Holdener BC, Percival CJ, Grady RC, Cameron DC, Berardinelli SJ, Zhang A, Neupane S, Takeuchi M, Jimenez-Vega JC, Uddin SMZ, et al. ADAMTS9 and ADAMTS20 are differentially affected by loss of B3GLCT in mouse model of Peters plus syndrome. *Hum Mol Genet*. 2019:**28**(24):4053–4066.

Houwen B. Blood Film Preparation and Staining Procedures. *Clin Lab Med*. 2002:**22**:1–14.

Hubmacher D, Schneider M, Berardinelli SJ, Takeuchi H, Willard B, Reinhardt DP, Haltiwanger RS, Apte SS. Unusual life cycle and impact on microfibril assembly of ADAMTS17, a secreted metalloprotease mutated in genetic eye disease. *Sci Rep*. 2017:**7**(1):41871.

Im JH, Muschel RJ. Protocol for murine/mouse platelets isolation and their reintroduction in vivo. *Bio Protoc*. 2017:**7**:e2132.

Iruela-Arispe ML, Liska DJ, Sage EH, Bornstein P. Differential expression of thrombospondin 1,2, and 3 during murine development. *Dev Dyn*. 1993:**197**(1):40–56.

Kale A, Rogers NM, Ghimire K. Thrombospondin-1 CD47 signalling: from mechanisms to medicine. *Int J Mol Sci*. 2021:**22**(8):4062.

Lawler J. The structural and functional properties of thrombospondin. *Blood*. 1986:**67**(5):1197–1209.

Lawler J, Chao FC, Cohen CM. Evidence for calcium-sensitive structure in platelet thrombospondin. Isolation and partial characterization of thrombospondin in the presence of calcium. *J Biol Chem*. 1982:**257**(20):12257–12265.

Lawler J, Derick LH, Connolly JE, Chen JH, Chao FC. The structure of human platelet thrombospondin. *J Biol Chem*. 1985:**260**(6):3762–3772.

Luca VC, Jude KM, Pierce NW, Nachury MV, Fischer S, Garcia KC. Structural biology. Structural basis for Notch1 engagement of Delta-like 4. *Science*. 2015:**346**:847–853.

Luca VC, Kim BC, Ge C, Kakuda S, Wu D, Roein-Peikar M, Haltiwanger RS, Zhu C, Ha T, Garcia KC. Notch-jagged complex structure implicates a catch bond in tuning ligand sensitivity. *Science*. 2017:**355**(6331):1320–1324.

Neupane S, Goto J, Berardinelli SJ, Ito A, Haltiwanger RS, Holdener BC. Hydrocephalus in mouse B3glct mutants is likely caused by defects in multiple B3GLCT substrates in ependymal cells and subcommissural organ. *Glycobiology*. 2021:**31**(8):988–1004.

Neupane S, Berardinelli SJ, Cameron DC, Grady RC, Komatsu DE, Percival CJ, Takeuchi M, Ito A, Liu TW, Nairn AV, et al. O-fucosylation of thrombospondin type 1 repeats is essential for ECM remodeling and signaling during bone development. *Matrix Biol*. 2022:**107**:77–96.

Perez-Riverol Y, Csordas A, Bai J, Bernal-Llinares M, Hewapathirana S, Kundu DJ, Inuganti A, Griss J, Mayer G, Eisenacher M, et al. The PRIDE database and related tools and resources in 2019: Improving support for quantification data. *Nucleic Acids Res*. 2019:**47**(D1):D442–D450.

Resovi A, Pinessi D, Chiorino G, Taraboletti G. Current understanding of the thrombospondin-1 interactome. *Matrix Biol*. 2014:**37**:83–91.

Santoro SA, Frazier WA. Isolation and characterization of thrombospondin. *Methods Enymol*. 1987:**144**:438–446.

Sanz S, Aquilini E, Tweedell RE, Verma G, Hamerly T, Hritzo B, Tripathi A, Machado M, Churcher TS, Rodrigues JA, et al. Protein O-fucosyltransferase 2 is not essential for plasmodium berghei development. *Front Cell Infect Microbiol*. 2019:**9**:238.

Sato T, Sato M, Kiyohara K, Sogabe M, Shikanai T, Kikuchi N, Togayachi A, Ishida H, Ito H, Kameyama A, et al. Molecular cloning and characterization of a novel human beta1,3-glucosyltransferase, which is localized at the endoplasmic reticulum and glucosylates O-linked fucosylglycan on thrombospondin type 1 repeat domain. *Glycobiology*. 2006:**16**(12):1194–1206.

Shcherbakova A, Preller M, Taft MH, Pujols J, Ventura S, Tiemann B, Buettner FF, Bakker H. C-mannosylation supports folding and enhances stability of thrombospondin repeats. *Elife*. 2019:**8**:e52978.

Sigoillot FD, King RW. Vigilance and validation: keys to success in RNAi screening. *ACS Chem Biol*. 2011:**6**:40–61.

Thomas M, Lu JJ, Ge Q, Zhang C, Chen J, Klibanov AM. Full deacylation of polyethylenimine dramatically boosts its gene delivery efficiency and specificity to mouse lung. *Proc Natl Acad Sci USA*. 2005:**102**(16):5679–5684.

Tiedt R, Schomber T, Hao-Shen H, Skoda RC. Pf4-Cre transgenic mice allow the generation of lineage-restricted gene knockouts for studying megakaryocyte and platelet function in vivo. *Blood*. 2007:**109**(4):1503–1506.

Tuszynski GP, Rothman VL, Deutch AH, Hamilton BK, Eyal J. Biological activities of peptides and peptide analogues derived from common sequences present in thrombospondin, properdin, and malarial proteins. *J Cell Biol*. 1992:**116**(1):209–217.

Vasudevan D, Takeuchi H, Johar SS, Majerus E, Haltiwanger RS. Peters plus syndrome mutations disrupt a noncanonical ER quality-control mechanism. *Curr Biol*. 2015:**25**(3):286–295.

Wang LW, Dlugosz M, Somerville RP, Raed M, Haltiwanger RS, Apte SS. O-fucosylation of thrombospondin type 1 repeats in ADAMTS-like-1/punctin-1 regulates secretion: Implications for the ADAMTS superfamily. *J Biol Chem*. 2007:**282**(23):17024–17031.

Wang J, Miao Y, Wicklein R, Sun Z, Wang J, Jude KM, Fernandes RA, Merrill SA, Wernig M, Garcia KC, et al. RTN4/NoGo-receptor binding to BAI adhesion-GPCRs regulates neuronal development. *Cell*. 2022:**185**(1):218.

Zhang A, Berardinelli SJ, Leonhard-Melief C, Vasudevan D, Liu TW, Taibi A, Giannone S, Apte SS, Holdener BC, Haltiwanger RS. O-Fucosylation of ADAMTSL2 is required for secretion and is impacted by geleophysic dysplasia-causing mutations. *J Biol Chem*. 2020:**295**(46):15742–15753.